Rev. Téc. Ing., Univ. Zulia
Vol. 6, Edición Especial, 1983

Neville F. Rieger
Stress Technology Incorporated
Rochester, New York, USA

SOME SERVICE PROBLEMS OF TURBINE BLADES : FACTORS AFFECTING DIAGNOSIS AND CORRECTION

*(Al Libertador Simón Bolívar,
en el bicentenario de su nacimiento)*

ABSTRACT

This paper discusses several important types of turbine blading failure. A review of the basic causes of blading failures, e.g. fatigue, corrosion, stress corrosion cracking, erosion, etc., is given. Procedures for calculating stresses associated with such failures and the number of cycles to failure are reviewed. The familiar Goodman diagram procedure for cycles to crack initation is included, plus a fracture mechanics approach to give the number of propagation cycles. Four case histories of turbine blade failure are described in detail, including operating conditions, diagnostic procedures used, determination of failure cause, and remedies chosen to avoid further blading failures, in each case. 13 references to the subject literature are given.

RESUMEN

En este trabajo se discuten varios tipos importantes de fallas de álabes de turbinas. Se revisan las causas fundamentales de dichas fallas, tales como fatiga, corrosión, ruptura por esfuerzos de corrosión, erosión, etc. También se revisan los procedimientos para el cálculo de los esfuerzos asociados a tales fallas y para el número de ciclos antes de la falla. Se incluye el conocido procedimiento del diagrama de Goodman para el cálculo del número de ciclos antes del comienzo de la ruptura, así como también una interpretación del mecanismo de ruptura que permite calcular el número de ciclos de propagación. Se describen en detalle cuatro casos de fallas de álabes de turbinas, incluyendo condiciones de operación, el procedimiento usado para el diagnóstico, la determinación de la causa de la falla y los remedios escogidos para impedir nuevas fallas en cada caso. Se dan 13 referencias bibliográficas.

INTRODUCTION

Service failures of turbine blades are infrequent but costly events. Electrical utility records show nearly 30 percent of all steam turbine forced outages are attributable to blade problems such as cracking, erosion, component fracture, etc. Blade-related turbine outages may range from several days for a simple blade replacement in a small unit, to several months downtime for a significant blading failure in a large unit with consequential damage. Outage duration is obviously influenced by the availability of replacement parts, as well as repair time. Similar circumstances apply to process drive turbines and to marine propulsion turbines.

This paper discusses several causes of steam turbine blading failures, with important factors relating to these failure causes. Corrective measures which have been used succesfully in the past to overcome such problems are indicated. Knowledge of potential problem areas and of corrective measures is of value to designers and turbine operators wishing to avoid similar problems in the future. Procedures for the analysis of stress-related blading failures involving both high-cycle and low-cycle fatigue are described. These procedures permit quantitative assessments to be made of cases involving major stress-related failure mechanisms such as fatigue, corrosion fatigue, and stress corrosion. Several case histories of blade failures are described, together with practical remedies which were used to overcome these failures.

Most blading problems present and unclear variety of evidence when the turbine is first opened. The first task is to carefully record and evaluate the failure data and operating conditions which the blading has experienced, when looking for the cause of a given problem. Identification of the failure cause is the first major step toward prescribing an effective solution. However, problem diagnosis may be a secondary objective in the period immediate following the failure. The turbine operator usually wants to 'get running'again, using some interim arrangement such as reblading with available replacements or removal of the damaged row. Properly utilized, this situation offers a valuable time-opportunity for thorough investigation and diagnosis of the problem as a basis for a more permanent fix to be installed at a futur outage.

BLADE LOADING CONDITIONS

The ability of a blade to support its applied loads depends on:

a. Strength of blade material in its environment

b. Magnitude and distribution of steady mean stresses

c. Magnitude and distribution of alterning stresses

d. Loading history, including power and overspeed conditions

Strength of the blade material is influenced by possible corrosive effects in the environment, by mean and alternating stress levels, by transient peak overload conditions, and by the number of applied load cycles. Turbine blades may be subject to complex three - dimensional stress conditions at their attachments to adjacent blades in the group, and at their attachments to the rim of the disk. Both the mean stresses and the alternating stresses have localized maximum values at such locations, ie at the cover-tenon junction, at the tie-wire attachments at certain locations in the airfoil section, at the airfolplatform junction, and in the blade root/disk attachment region. The mean stress value depends on centrifugal and steam loading conditions. Alternating stresses result from steam (and other) dynamic stimuli, from the modal response properties of the blade group, from the degree of modal damping involved, and from the extent of the dynamic coupling which occurs between the stimulus and the blade group modes. Loading history involves such factors as overspeed events, base load operation vs. peaking operation, and machine MWe load profile. It also may involve more subtle dynamic factors such as circumferential pressure distribution resulting from exhaust hood geometry, from reheat/extraction port locations, size, and arrangements, and from manifold strut-arrangements, water ingestion, condenser vacuum rupture, and electrical line-switching transient conditions.

DIAGNOSIS OF FAILURE MECHANISM

A variety of vibration sources may exist within a turbine stage, but in most instances the resulting blade vibration amplitudes and associated stress levels are small and insignificant. Occasional cases have been observed where the vibration amplitudes of blades were shown to be large enough to have caused blade failure by fatigue. More frequently, blade vibration plus some other significant factor, eg corrosion, residual stresses, was involved. Correct diagnosis of the failure mechanism is necessary before modifications can be proposed with confidence. The following questions may provide useful information when seeking the cause (s) of a given blade failure:

a. Does the evidence suggest that failure was due to (i) high cycle fatigue, (ii) low cycle fatigue, (iii) stress corrosion, (iv) corrosion assisted fatigue, (v) erosion, (vi) creep, (vii) other sources, eg water ingestion?

b. What were the tangential, axial, and group natural frequencies of the blades under operating conditions? What were the associated mode shapes?

c. Was resonance possible between any blade group mode and any per-rev excitation harmonic (1x, 2x, etc.)?

d. Was resonance possible between any blade group mode and any harmonic of nozzle-passing frequency (1 x NPF, 2 x NPF, -----)

e. Where was the failure initation site located. Was there evidence of local damage from corrosion, erosion, impact, or other initiating cause in that region?

f. What are the operating load and speed cycle history details for the machine since the original spin pit proving tests? How many overspeed governor trips have occurred? What speeds were reached in such cases?

g. What was the chemical history of the steam operating conditions. Where was this sampled?

Other considerations such as location of Wilson line in the machine, electrical network load variation details, and unit thermal cycling profile details may also be important. Some known features of several important blade failure mechanism are discussed in the following section. It is evident that monitoring of speed and load to identify any transient conditions can provide important diagnostic information in such instances.

TYPES OF BLADING PROBLEMS

A. Fatigue

Fatigue in turbine blades is broadly classified as either high-cycle fatigue or low-cycle fatigue. High-cycle fatigue is generally associated with a high mean stress level and moderate dynamic stresses. With high-cycle fatigue, a large portion of the time to failure is taken up with the initation of the fatigue crack. When a crack develops, the stresses at the crack front are much increased, and crack propagation usually takes place quite rapidly under the same alternating blade load which caused the crack to initiate.

Low-cycle fatigue is commonly associated with fewer load cycles applied through a much larger stress range than that which occurs with high-cycle fatigue. A typical low-cycle fatigue would be from zero to maximun stress, such as the star-stop cycling of a blade or disk to centrifugal force. For any turbine blade in which the local maximum stress exceeds the material yield point during the load cycles will be needed to cause a crack to initiate (and subsequently to propagate) compared with the cracking and propagation rates observed in high-cycle fatigue.

Many sources of harmonic stress exist in turbine blade applications. Steady harmonic excitations are continously applied to the blades from many sources such as nozzle wake excitations. Under resonant conditions, these excitations may cause large dynamic stresses to occur in a blade due to the low damping which exists in most turbine blades. Transient blade excitations of large magnitude may also occur, and cause transient vibration stresses to occur. Such transients may arise from network electrical fault conditions at the generator, or from partial steam admission on start-up, and so on. Intermittent blade vibrations evidently tend to cause slower overall crack growth rates, but the growth increment can be larger where large dynamic stresses are involved.

High-cycle fatigue failures can usually be recognized by visual inspection from the characteristic pattern of lines (called beach marks) which radiate from the fatigue crack site. The surface may be uniformly polished from the rubbing of the crack surfaces against each other during vibration. The surface may also be tinted, depending on whether corrosion has ocurred from the gas/steam environment. Frequently there is intermittent growth of the fatigue surface. This indicates intermittent growth of the fatigue crack, showing that crack-driving excitation was not constantly applied throughout the blade fatigue life. See figure 1.

Many high-cycle blade fatigue failures originate at some structural discontinuity or stress raiser. Such failures are frequently related to steady high local stresses, eg. from centrifugal blade loading, as well as dynamic stresses. With high steady stresses, more moderate vibratory stresses may cause a crack to initiate and propagate from the stress raiser. The same conditions can also cause an existing crack to propagate and grow until the component fails.

Low-cycle turbine blade fatigue failures are frequently associated with corrosion or high temperature. The influence of these effects on fatigue is discussed later. Where cyclic stresses alone have led to low-cycle fatigue failure, the progressive development of the crack can often be seen from electron microscope photographs, figure 2.

B. Corrosion

Corrosion-assisted failures have occurred in blade roots and in disk steeples, and in the vane, tie wire, tenon and cover sections of the blade. Such failures typically occur at points of high operating stresses: The presence of dynamic stress is not required for stress-corrosion failure to occur. Corrosion fatigue may also occur where large dynamic stresses are applied. This is discussed in the next section.

Corrosive attack on blade and disk materials arises from chemical impurities in the steam, such as sodium and potasium chlorides, sulphides and carbonates. These substances usually exist in the steam in small quantities. Efforts are made to reduce chemical impurities by water treatment. The effect of even very small quantities (parts per billion) may be concentrated by entrapment in grooves and cracks. Where such entrapment occurs at or near high-stress regions, stress corrosion may result. Evidence of concentrated corrosive attack may range from general degredation of the surface quality to corrosion failure of a component. See figure 3.

Corrosion coupled with component stress and steam/erosion may result in sufficient deterioration of a blade airfoil surface to affect the operating performance over a period of time. corrosive build-up of deposits on blade surfaces can adversely affect stage operating efficiency by several percent. This has occurred in large, utility steam turbines, process turbines and geothermal steam turbines. Stress - accelerated breakdown of surface condition is another important practical source of turbine blade degradation.

The possibility of stress corrosion cracking and failure of a given component may be assessed by fracture mechanics procedures. Visual data which suggests this type of failure are the presence of white or gray chloride, sulphide, and/or carbonate deposit (nodules) generally coating the surfaces (moving and stationary blades). Signs of corrosive pits (small or large) may be evident especially near known regions of high stress, eg. notches. Additional data can be obtained from microscopic examination of the same surfaces, fig. 3. This may reveal additional corrosive degredation of the surface, and a variety of small and large pits. Medium -power microscope studies of sections through the surface may reveal that the progress of the crack has been aided by corrosive attack along the grain boundaries (intergranular cracking). The most informative source of such data is photographs from the scanning electron microscope which reveals the presence of corrosive attack as large nodules of corrosion products in such pictures. See case Histories.

A recent paper by Jonas (1), discusses the general problem of corrosive attack on components from steam impurities. Table 2 herewith is taken from this paper. It identifies the locations, component materials, and associated chemical deposits observed at the sites of a variety of turbine plant problems. Three regions are specified as most susceptible to corrosion. (a) Regions where metal or steam temperatures are around the melting points of corrodents, eg. NaOH T_m = 604°F. (b) Regions immediately ahead of, or at first condensation, eg. LP turbine stage at Wilson point. (Pitting, stress corrosion, and corrosion fatigue of blades and disks occurs most often in this region.) (c) Superheated metal surfaces where impurities can concentrate by evaporation and drying. Longterm (24,000 hours) tests (1) on certain turbine steels at 150°F in a 28 percent NaOH, solution, have shown that stress corrosion cracking may occur at stresses around 30 percent of the material yield strenght.

Recent utility turbine research programs have begun to develop comprehensive methods for chemical monitoring of steam turbine plants. A useful description of appropiate tests and water/steam monitoring requirements is given in the above paper by Jonas.

C. Corrosion Fatigue

Corrosion-assisted fatigue is probably the major source of steam turbine blade fatigue failures. Corrosion fatigue may occur in a corrosive environment where high steady stresses are applied together with high alternating stresses. Turbine blade vibration tests by many investigators have shown that even under conditions of nozzle resonance, blade types which have been known to fail during operation usually do not develop dynamic stresses of sufficient magnitude for resonant fatigue alone to appear as an obvious cause of the failure under investigation. Such conditions suggest that some other factor must be involved, and these failures can frequently be explained where it can also be shown that significant corrosive attack has occurred along with fatigue conditions in the same operating enviroment. Laboratory test evidence has demonstrated that the material fatigue strength (endurance limit) may be reduced in the order of seventy percent by a sufficiently aggressive chemical environment. On occassions, such chemical environments appear to have existed in, (a) certain marine turbine steam conditions, eg. from sodium hydroxide in the make-up water, (b) from inadequate demineralizers in main utility stations, and (c) from ground water infiltration into condensers in process steam turbines. Otherwise unexplainable blade fatigue failures can be accounted for quite readily where such circumstances can be shown to have existed for a sustained period. Corrosive enviroments may accelerate both high-cycle fatigue and low-cycle fatigue if the operating conditions and chemical concentrating mechanism are right.

Corrosion fatigue in turbine blade steels has been studied in depth in recent years, and certain fracture mechanics data have been given, eg. by Clark (2). Figure 4 shows the rate of crack growth da/dN vs. stress intensity factor ΔK for a 304 stainless steel in a three percent caustic environment. Crack growth for the same steel in air is also shown for comparison. It is seen that the difference in crack growth rates for the same ΔK value, ie. stress level, is approximately 3:1 for the caustic environment. This is another way of stating that the fatigue strength of the test components under the corrosive attack shown in this instance was only about one-third of the fatigue strength of the same components in air.

An important initial source of corrosion fatigue may occur on-site when rotors are left exposed to the environment for long periods prior to erection. Particularly damaging is the case where the protective coating has been removed from a rotor and blades, which are then left exposed to the moist, outdoor environment near a river or even the sea. The initial chloride pitting which may occur in such circumstances may later provide nesting sites for steam, etc, impurities in high-stress regions which can accelerate the tendency toward blade fatigue.

D. Erosion

Surface erosion can be a significant problem in all stages of a turbine. Surface erosion from hard particles (usually boiler exfoliation) can damage the H.P. and I.P. stage blading, and wet steam erosion can damage the leading edge of the long blades, usually from mid-height out to the cover. Cover damage from wet steam erosion can also be significant. Such erosion is caused by high-velocity water particles striking the blade lead edge over a period of time and eroding the material away. Certain wet region blades have been designed for many years with an erosion shield (stellite strip), which is bronze welded on to the blade lead edge to protect against wet steam erosion.

Signs of early erosion may often be observed on those blade leading edges which project noticeably out into the oncoming steam, beyond the other blades in the same row. This condition may occur from minor misalignment on assembly, and this erosion is of no special significance unless it continues and presents an evident major damage problem. Replacement of damaged erosion shields is a straight-forward procedure which can now be undertaken in the field, as well as in the manufacturer's shop. Suitably-located LP moisture separators can help to decrease the rate of blading erosion.

Exfoliation of tube scale is another form of erosion which occurs in boiler tubes, superheater tubes, inlet steam pipes, and from condenser pipes. The scale develops from oxidation and corrosive attack from the feed water condensate and from steam impurities. The scale is eroded away, and on passing the turbine, may damage the blading and may accumulate in the drains. Geothermal turbines are especially prone to scaling and exfoliation damage because of the high corrosive and impurity content of the inlet steam. Erosion products should be monitored as part of the turbine system chemical monitoring program.

STRESS RELATED BLADE GROUP CRACKING THEORY

The following theoretical approach is general and may be used to develop quantitative data for specific cases of blade cracking which appear to involve fatigue, corrosion fatigue, or stress corrosion cracking. It follows from the Prohl(3) method.

Consider a group of blades rotating in an axial flow turbine, figure 6. The total stress at any location is due to two sources, the steady mean stress σ_m and the dynamic or alternating stress σ_a At any instant during operation, this total stress is given by:

$$\sigma_t = \sigma_m + \sigma_a \cos\omega t \, ,$$

where ω is the circular frequency of the alternating stress. The mean stress results from the combined action of the centrifugal load due to turbine rotation, and from the steady blade bending load from the gas forces which drive the turbine.* These mean stress components combine to give the nominal steady extreme fiber stress, σ_{mo} at the blade (or root) section:

* Additional forces from torsion, centrifugal untwist, etc. may also apply.

$$\sigma_{mo} = \sigma_{co} + \sigma_{bo} = P/A + Mc/I$$

where P is the centrifugal load at the section, A is the section area, M is the local bending moment due to the gas force, c is the extreme fiber distance from the neutral axis, I is the appropiate second moment of area of the blade section, and σ_{co} and σ_{bo} are the nominal centrifugal and bending stresses at the section (no stress concentration effects). The mean stress remains constant for a given blade arrangement at specified speed and power output. Corresponding expressions may be written for steady stresses in the cover and tenons.

Alternating stresses in the blade may arise from several causes, of which harmonic excitation from the nozzle wakes is recognized as a potentially significant contributor. The frequency of excitation f from the nozzle wakes is given by

$$f = Nk = 2\pi\omega \text{ cycles/sec (Hz.)}$$

where N is the rotor speed rev/sec and k is the number of uniformly spaced nozzles ** around the 360-degree circumference. Alternating stresses from nozzle excitation depend on several factors:

a. The magnitude of the gas exciting force or harmonic stimulus, expressed as a stimulus factor S.

b. The damping of the blade and its attachment expressed as a logarithmic decrement δ.

c. The resonant response factor K which is a measure of the ability of the blade group to accept energy input from the nozzle stimulus.

Blade harmonic stimulus is expressed as a proportion of the steady gas bending force F acting on the blade, ie. $S = \Delta F/F$, where ΔF is the amplitude of the time-varying gas force acting on the blade. In practice, values of S may range from below 0.05 in smooth-running stages to above 0.30 in rough stages with off-optimum conditions. See references (4) and (5).

Damping in blade groups can arise from several sources such as rubbing friction in the attachment areas (root, cover), from material hysteresis and from gasdynamic effects on longer blades. The magnitude of blade group logarithmic damping value δ may vary substantially from one application to another, but the general range is from about 0.002 to 0.030 for conventional AISI 403, 12 chrome steam turbine blades, depending on blade geometry and the mode of vibration involved. See references (6) and (7).

The resonant response factor K depends on the excitation parameter $E = (nk/m)$, where n is the harmonic number (n = 1, first order; n = 2 second order, etc.), k is the number of nozzle inlets and m is the number of blades. The variation of resonant factor k represents conditions under which the blade group will receive strong energy input from the nozzle stimulus and the blade vibrations are not readily excited in this condition.

As each turbine stage may contain many excitation harmonics, and each harmonic may act on several blade group modes, the influence of the excitation parameter on each blade group response in the frequency ranges of interest should be examined. A convenient procedure for determining the excitation harmonics and blade modes of interest was first given by Campbell (8) in which the natural frequencies of these modes are plotted as ordinates and the rotor speed is plotted as abcissa, see figure . Radial lines from the origin corresponding to once-per-rev (1x), twice-per-rev (2x), etc. nozzle passing frequency (Nk), twice-NPF (2nk), etc. are also plotted. Speed regions of intersection between blade frequencies and excitation harmonics are then noted, with particular reference to regions of sustained operation, eg. operating speed range. The Campbell diagram shown in figure 9, indicates the possibility of blade resonance in the axial-torsional mode with the twice NPF excitation, and also excitation of the second-type tangential mode by NPF. See case History Number 1 for details.

Resonant stresses are related to stimulus S, damping δ, and blade group dynamic response factor K, by the expression:

$$\sigma_{ao} = \frac{\Pi}{\delta} K \, S \, \sigma_{bo}$$

where σ_{ao} is the nominal resonant alternating extreme fiber stress at the blade (or root) section, and the σ_{bo} is the nominal bending stress at the section, defined previously. It is evident that the practical combinations of blade damping, nozzle stimulus, and dynamic response factor may lead to resonant stresses σ_{ao} at certain blade cross sections which could approach or greatly exceed the nominal mean bending stress σ_{bo} at that section. It should further be noted that in practice, the resonant condition is often sharply defined. Sustained operation at the resonant peak condition is therefore unlikely to occur for long periods, though some lesser stress magnification should always be expected for operation in this region.

To determine whether the stress conditions at a given location could be responsible for blade cracking during operation, it is necessary to compare the local stresses with the appropiate strength criterion for the blade material at that section. To find whether the nominal stresses σ_{ao} and σ_{bo} are likely to initiate high-cycle fatigue cracking, a procedure due to Heywood (9), Rieger and Nowak (10), which uses the Goodman diagram may be used as follows. The fatigue envelope for unnotched specimens is modified in a specified manner to account for mean stress, local stress raisers,

---

** k may also be considered as the number of harmonic cycles around the circumference. This allows per-rev nozzle excitations to be considered.

cycles to failure, and size effect. The new (notched, etc.) fatigue envelope then becomes the crack initiation criterion against which the nominal stresses σ_{mo} and σ_{ao} are compared. A point falling outside this region can be expected to initiate a crack in the number of cycles assumed in the calculation of the notched envelope, ie $N = 10^4 \ldots 10^5 \ldots 10^7$, etc. For high-cycle fatigue, crack initiation commonly represents the larger portion of the fracture life, and the time to propagate the crack (which is not considered in this approach) represents the remainder of the component life.

Where the initial defect size is known from inspection, an alternate approach using fracture mechaniscs procedures may be used to estimate the number of load cycles required to propagate a crack from the defect, and cause failure of the defective component. Suitable materials data obtained from tests on fracture mechanics specimens tested with a similar environment and loading, in accordance with standard ASTM testing procedures, is required. The rate of crack propagation da/dN is related to material properties A, n, stress intensity range ΔK, and applied stress ratio by the expression:

$$\frac{da}{dN} = \frac{A\left[\Delta K\right]^n}{(1-R)^{0.5}}$$

ΔK is the range of stress intensity factor= $c\Delta\sigma\sqrt{\pi a}$

R is the stress ratio, Kmin/Kmax or $\sigma_{min}/\sigma_{max}$

A,n are material properties

C is a geometric factor for the crack model involved

$\Delta\sigma$ is the stress range, $\sigma_{max}-\sigma_{min}$

a is the crack length

N is the number of stress cycles

For a crack in a notch-free region,

$$\sigma_{max} = \sigma_{mo} + \sigma_{ao}$$

$$\sigma_{min} = \sigma_{mo} - \sigma_{ao}$$

$$\Delta\sigma = 2\sigma_{ao}$$

$$R = \sigma_{min}/\sigma_{max}$$

For a crack in a sharply-notched region,

$$\sigma_{max} = K_t^m\sigma_{mo} + K_t^a\sigma_{ao}$$

$$\sigma_{min} = K_t^m\sigma_{mo} - K_t^a\sigma_{ac}$$

$$\Delta\sigma = 2K_t^a\sigma_{ao}$$

$$R = \sigma_{min}/\sigma_{max}$$

σ_{max} and σ_{min} are the maximum and minimum values of the total stress at the location in question. A typical relation between da/dN and ΔK for a 4340 steel in a three-percent caustic solution is shown in figure 4. This chart does not include the effect of mean stress ratio R. In most cases the stress field in the body changes with distance into the body. This causes the stress at the crack tip to change and so influences the rate of crack propagation. Calculations with each of the above factors which must include the effect of variation are most conveniently performed with a suitable fracture mechanics computer program, such as the CRACKS (11) or BIGIF (12). The end result of such a calculation is a value for a specific number of cycles to propagate the crack, either to failure when Kmax = K_{IC} (fatigue) or K_{ISCC} (corrosion fatigue), or until a length is reached at which the crack stops propagating.

This fracture mechanics procedure is suitable for failure analysis at any location in the blade group with a crack of known (or assumed) proportions, and for any material for which suitable fracture mechanics data is available for the blade operating environment. Where such input data is difficult to obtain or specify, the above procedure may be used to provide a bounding analysis suitable for determining the performance of a hypothetical crack under assumed minimum or maximum stress and material conditions.

CASE HISTORIES OF BLADE FAILURES

Case 1. Nozzle Resonance Fatigue of HP Marine Turbines, Ref. (13)

Both rotors were 55,000 SHP turbines operating at 3500 rpm. The blading of both HP rotors sustained damage. The complete blading of the 9th stage of the starboard turbine was missing and eight blades were missing from stage 10. On the port rotor, seven blades were missing from the 9th stage and there was some cracking in stages 8 and 10. The cracks occurred near the vane-platform junction where the vane overhung the platform. In most instances the cracks appeared to have propagated from beneath the overhung trailing edge, horizontally into the vane airfoil section, figure 7(a). One blade only was broken at mid-height, in the 8th stage of the port turbine.

A comprehensive investigation was made of the failure. Frequency calculations and vibration tests were performed on the original blades, and on the modified blades. Much evidence was found to show that the failures were due to high-cycle fatigue from vibrations in the second-type tangential (out-of-phase) mode, figure 8(a). The cracking pattern correspondend to the calculated distribution of modal amplitudes shown, both in magnitude and location. The Campbell diagram figure 9, showed that the 8th, 9th, and 10th stages could resonate at propeller shaft speeds between 90 rpm and 174 rpm. The ship operating log, fig. 10, showed 2610 minutes of operation at 148 rpm. In this condition, the 9th stage could resonate in its second tangential mode.

The overhang stress raiser was eliminated by smoothing the vane into the platform in the replacement blades, figure 7(b). Tie-wires were added by brazing to eliminate the second tangential mode from the range of nozzle resonance, fig. 8(b). Diaphragm changes (decreased number of nozzles) were also considered, but were not used because such changes were shown to be effective in removing the 8th stage alone from resonance. Also, larger nozzle passages frequently lead to higuer exciting forces.

Case 2. Nozzle Resonance in 9th Stage of Process Steam Turbine.

A rash of shroud and vane cracking incidents had occurred in several process turbine drive units. Generally the shroud of a six-blade group had cracked, and also several vane sections near the platform in the 8th stage of the drive turbine units had cracked. The blade surface adjacent to the failure site was pitted, and white, solid deposits of unknown type were attached to the blade surface. A diaphagm change from 34-inlet nozzles to 46-inlet nozzles had increased the blade life somewhat (6 weeks to 40 weeks), but had not eliminated the problem.

Analysis showed that the second in-phase tangential mode of the blade group coincided with NPF at full operating speed with the 34- nozzle diaphragm. Further, the Campbell diagram, figure 11, showed that although a change from 34-nozzle openings would cease to excite the second in-phase tangential group mode with the second HPF harmonic (2x34), the (1x46) NPF harmonic would then excite several second-type tangential (out-of-phase) modes.

The fix proposed in this instance was a blade profile redesign which removed the blade groups from the troublesome resonance harmonics within the operating speed range identified above, without introducing other resonance problems. The blades were also detuned as shown in fig. 12, so that E would be 0.183 and the corresponding response factor K would become zero. In the original design, E was 0.352 and the resonant response factor K had been 0.275. The new blades were therefore less responsive to nozzle stimulus.

Further factors requiring attention were the chemical content of the steam and the location of the Wilson point in the turbine. Suitable demineralizers should have been prescribed and thoroughly maintained in view of the corrosion-fatigue situation which existed. If the Wilson point corr sponds to the 9th stage, care should be taken to shield the attachment areas in some manner. The chemical functioning of the turbine steam system should have been monitored following the reinstallation to ensure that solids and impurities were within acceptable limits. See Jonas (1).

An apparent alternate fix would have been to detune the blades using a bronze welded tie-wire, as was done in Case 1. This would suppress the out-of-phase tangential modes, and the 46-nozzle diaphragm would not excite the second in-phase tangential mode, as noted. This was not done as the blade required redesign to remove the vane overhang.

Case 3. Stress Corrosion in a 5th Stage 200MW Utility Turbine.

Catastrophic rupture occurred in the blade root section of thirteen 5th stage axial entry blades after 11 months of on-line operation, with considerable consequential damage to flow guides and to blades in adjacent stages. The failed row contained 324 moving blades, each about six inches average vane height, arranged in groups of five and six blades. Blade material was 403 stainless steel with UTS 105 KSI, and yield stress 85 KSI, approximately. The adjacent inlet nozzle row had 240 nozzles. Extensive white-colored chemical deposits with average ph value of 11, coated the general region (nozzles, moving rows), near the failed stage, figure 13. Pitting in the remaining blades of the row ranged from slight to severe. 325 additional cracks were found (173 blade, 152 disk steeples), of varying sizes, mainly in the contact hook regions of the blade attachments. The location of the row coincided with the location of the Wilson point (dry/wet) of the rotor at full power.

Metallographic examination showed intergranular cracking and some branched intergranular cracking inward from the highly stressed blade root notch surface, figure 14. Scanning electron microscope studies showed pitting in the vicinity of the primary fractures and secondary intergranular fractures linking the corrosion pits. The fracture surfaces were relatively clean, indicating that little rubbing or polishing had taken place since clevage occurred. This suggests that no significant fatigue or dynamic stress mechanism was involved. The high-ph, white coating were composed of NaOH, and Na_2CO_3. This indicates that the initial cracking had been assisted by corrosion in the highly stressed hook region of the blade root. Furthermore, The original material away from the corrosion sites still had the strength and impact properties required in the original material specifications. A typical SEM photograph of the fracture surface is shown in figure 15.

Further investigation revealed that the boiler feedwater chemistry during operation had contained dissolved solids, iron, and sodium (77 ppb compared with 30 ppb specified), in excess of prescribed limits, despite the use of feedwater demineralizers. Stress corrosion of the blade root material under high stress conditions was the primary cause of this blade failure, based on (a) high sodium and other salt deposits, (b) wet/dry Wilson point at failure location, (c) widespread cracking in the vicinity of the high stress locations, (d) general pitting of adjacent surfaces, (e) absence of plastic flow and beach marks on the failure surface, (f) corrosion products seen in many SEM scans, and (g) corrosion fractography observed in sectioned failure regions. The principle remedy was improved steam quality and boiler feedwater chemistry by improved demineralizer control and monitoring.

Case 4. Fatigue Failure of 4th Stage Marine LP Turbine Impulse Blades.

A single side-entry 4th stage blade failed catastrophically in the root section at the first hook after 13 months of service at sea. On inspection it was found that 11 additional 4th stage blades were also cracked in the same region, and that all cracked blades were end blades of seven-blade groups. In addition, a total of eight disk root sections were found to be cracked in the same stage. These failures were found by magnetic particle inspection. Hardness and chemistry checks of the blade and disk root sections were also made. Hardness was found to be in the RC 20-21 average, as required. Macro-etched sections of the cracked root were carefully inspected at 20x magnification.

The failure mechanism was found to be fatigue. This was indicated by the progressive beach-mark crack progression along several regions of the failed surface. The multiple crack origins indicate a wide distribution of the initial crack-driving stress mechanism along the root hook notch. No oxides or corrosive deposits were observed on the fracture surface. Microexamination showed that the root cracks were relatively straight and intergranular without branching. This further suggests that pure fatigue was the cause of failure, though no electron microscope studies were made on this occasion.

Several possible causes of these fatigue failures were identified. First, the tangential out-of-phase group modes were found to lie close to nozzle resonance, due to an inaccurate design estimate of blade root stiffness. Second, the root fillet radius of 0.031 incles was quite small, and this gave rise to high fillet stresses. Third, variations in nozzle geometry from stage arrangement around the nozzle row were found to give 4:1 variations in the magnitude of nozzle stimulus. This raises the additional possibility of per-rev stimulus from this nozzle geometry variation, but this possibly was not considered further. Fourth, a small amount of stress corrosion may have occurred judging from minor discoloration observed on the crack surface. Fifth, a further source og significant excitation was thought to have occurred from four condensate extraction ports located around the circumference, adjacent to the 4th stage moving blade row.

Design modifications were made as follows: (1) Long-arc shrouding was introduced to suppress the troublesome resonant group modes. (2) The notch fillet radio were increased to 0.060 inches to reduce the fillet stresses. (3) The inlet nozzle geometry was made uniform around the diaphragm and the number of inlet nozzles was increased from 92 to 120. (4) A flow-smoothing baffle was inserted to remove the flow disturbances created by the four extraction openings. No further failures have occurred since the introduction of these modifications.

CONCLUSIONS

1. Turbine blade problems may occur due to causes of design, manufacure, materials properties, steam/gas quality (erosion), steam/gas chemistry (corrosion, exfoliation), and abusive operation (water extraction, condenser flooding). Design practices, operating practices, and turbine plant specifications should address each of these potential problem areas.

2. The primary diagnostic tools for analysis of turbine blade failure causes are:

(a) Electron microscope to investigate failure mechanism and identify the role of corrosion in the failure.

(b) Surface microscopy and section microscopy for defining the cracking mechanism, and for basic material quality assessment.

(c) Water/steam chemistry records to determine role of corrosion.

(d) Blade group, disk natural frequencies, modes and static/dynamic stress calculations, to determine role of operating stresses.

(e) Fracture mechanics testing of failed component material to determine quality of material supplied, corrosion resistance, and crack propagation characteristics in operating environment.

3. The failure surface and fracture sections should always be examined microscopically when the causes of a failure are being sought. Examination by Scanning Electron Microscope is a valuable additional aid for determining whether the failure is associated with corrosion, corrosion fatigue, or fatigue alone.

4. Each stage of blading should be checked as to whether nozzle resonance and per-rev resonance may occur during operation. A Campbell diagram should be developed containing the first six modes of the blade group for each stage. The calculated modes and frequencies should be checked by vibration tests performed in the manufacturer's shop, on several blade groups around the circumference of each stage.

5. High-cycle fatigue is usually related to some resonant operating condition. HCF may be identified by the presence of polishing, beach marks, crack propagation increments under SEM, and final static rupture on the failure surface. Multiple staining lines indicate the occurrence of intermittent crack propagation from short periods of high dynamic stresses.

6. Corrosion fatigue may be induced by concentration of steam impurities acting on high-stress regions in the presence of dynamic stresses. The source of such corrodants may be in the steam itself, in the steam chemistry control apparatus, in the steam chemistry specifications, or in the original turbine erection environment.

7. Erosion of turbine blades and stage inlet

guides may occur from boiler and tube exfoliation, and from wet steam impact. Such erosion may lead to performance degredation, and to degredation and failure of the working components.

REFERENCES

1. Jonas, O.: "*Turbine Steam Purity*". Combustion Magazine, December 1978, p. 11.

2. Clark Jr., W.G.: "*Evaluation of the Fatigue Crack Initiation Properties of Type 403 Stainless Steel in Air and Steam Environments*". ASTM STP 559, American Society for Testing and Materials 1974, pp. 205-224.

3. Prohl, M.A.: "*A Method for Calculating Vibration Frequency and Stress of a Banded Group of Turbine Buckets*". Trans. ASME January 1958, pp. 169-180.

4. Heyman, F.J.: "*Turbine Blade Vibrations Due to Nozzle Wakes*", ASME Publication Paper Number 68 -WA/PWR-1. Presented December 1-5, 1968.

5. Rieger, N.F. and Wicks, A.L.: "*Non-Steady Force Measuremets and Observations of Flow in Three Turbine Stage Geometries*". Journal of Engineering Power, October 1978, Vol. 100, p. 525.

6. Lazan, B.J.: Damping of Materials and Members in Structural Mechanics, Pergammon Press, Inc., New York, 1968.

7. Wagner, J.T.: "*Blade Damping Tests*". Westinghouse Engineering Report EC-401, NOB S N00024-67-C-5494, May 1969.

8. Campbell, W.: "*Tangential Vibration of Steam Turbine Buckets*". Transcript of ASME, 1925 pp. 643-671.

9. Heywood: Designing Against Fatigue of Materials, Reinhold Publishers, London, England, 1962.

10. Rieger, N.F. and Nowak. W.J.: "*Analysis of fatigue Stresses in Turbine Blade Groups*". Workshop on Improved Turbine Availability, Electric Power Research Institute, Palo Alto, California, January 1977.

11. CRACKS: "*A Fortran IV Digital Computer Program for Crack Propagation Analysis*". USAF Flight Dynamics Laboratory, Wright - Patterson AFB, Dayton, Ohio, March 1970.

12. BIGIF: "*Fracture Mechanics Code for Structures*" Program User's Manual, Failure Analysis Associates, Palo Alto, California, December 1978.

13. Fleeting, R. and Coats, R.: "*Blade Failures in the HP Turbines of R.M.S. Queen Elizabeth 2 and Their Rectification*". Transcript Institute of Marine Engineers, London, England, October 28, 1969.

Tema 11 *Recibido el 25 de marzo de 1983*

TABLE 1: Possible Causes of Turbine Blade Failures

Failure Mechanism	Source	Location
Fatigue	Unsymmetrical stage flow Nozzle resonance Partial admission Torsional transients Negative sequence currents Excessive condenser pressure	General
Corrosion	Excessive corrosion agents in steam/feedwater.	General
	Concentration mechanism	Wilson line
Corrosion Fatigue	Corrosion plus vibration source	General
Erosion	Wet steam	LP stages Erosion shield, cover. Downstream of Wilson line.
Ash Deposit Scaling	Combustion residue in gas stream	Blade lead edge
	Boiler, pipewall exfoliation	HP stages
Water Ingestion	Moisture separators Condenser	Adjacent LP stages

TABLE 2: Industry Experience-Stress Corrosion & Corrosion Fatigue, Jonas [1].

Part	Material	Y.S., KSI	Environment
Pipe expansion joints	Inconel 600	35	Melted caustic,
	304 SS	30	611 to 710°C
HP turbine bolts	Re 26	—	High sodium in
	Pyromet 860	—	deposits
	Steel	—	—
	Incoloy	—	NaOH-NaCl in deposits
LP stationary blades	Welded 304	—	Na,K,Cl identified in cracks
LP stationary blades	304	30	Caustic & chlorides
IP rotating blades	Re 26	—	Caustic in steam and deposits
LP rotor	1Cr 1Mo 1/4V	87	Caustic carry-over, 140°F, 3 psi at saturation
Wheel dovetails in boiler feed pump turbines	NiCrMoV	97	Caustic in deposits
Shrunk on wheels	1Cr 1/2Mo	123	Caustic wash
Shrunk on discs	3Cr 1/2Mo	117	Up to 215 ppm of sodium hydroxide in boilers
Small turbine rotor discs	CrMoV	126, 133	Caustic and chloride in deposits
HP inner cylinder Horiz. Joints	—	—	—
HP rotor dovetails	CrMoV	—	Hydrogen sulfide (229 ppb in condensate) from sodium sulfite treatment
LP rotor	NiMoV	—	
HP discs	NiCrMo	117	Caustic from demineralizer in deposit
HP blade pins	Re 26	—	High caustic in feedwater, steam & deposits source: demineralizers
HP seal springs	Inconel 718	—	
HP bolts	AISI 4130	—	
LP discs	NiCrMoV	—	
HP inner cylinder Horizontal joints	CrMoV	—	NaOH, NaCl in deposits Source: demineralizers
Two LP discs (ESCOM)	2% NiCrMoV	114	—
Four LP discs (SECV)	2% NiCrMoV	114	—
Two LP discs	NiCrMoV	130	Caustic suspected'
Last minus one rotating blades (fossil turbine)	12 Cr, 17-4PH	—	Chlorides & sulfates in deposits
Single cylinder of a small turbine	Cast iron	—	High oxygen and sulphuric acid from hydrolyzed Na_2SO_4 plus oxygen
LP blades	12 Cr	—	
First row LP	12 Cr	—	Mixture of organic acids and acetic acid
LP discs and blade fastenings	Low alloy steel	—	
LP blades and shrouds (magnox reactor unit)	Stainless steel	—	Organic acids (acetic, propionic, butyric) from surface cooling water organic compounds (humic acids)
Last row LP rotating blades	12 Cr hardened	—	Inorganic acids in steam, ferrous chloride and sulfate in deposits
Stationary blades		—	Hydrochloric acid in steam (seawater cooling + powdex)

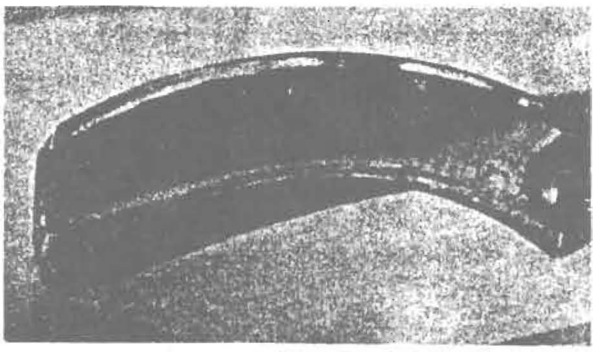

FIGURE 1. FATIGUE SURFACE WITH STAINING PATTERN.

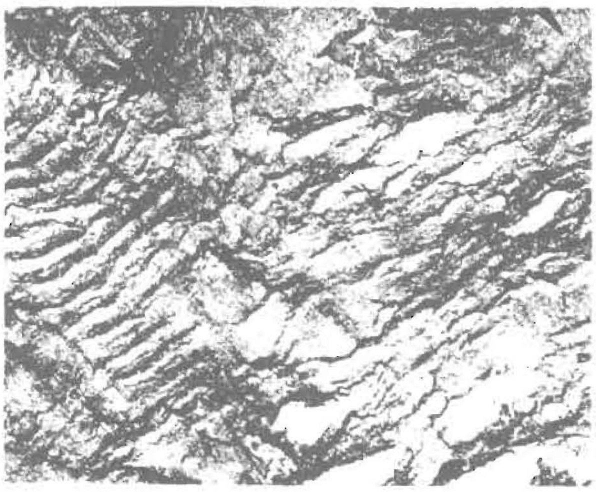

FIGURE 2. ELECTRON MICROGRAPH SHOWING FATIGUE STRIATIONS IN 4340 STEEL (BEACHAM,PELLOUX,REF.20).

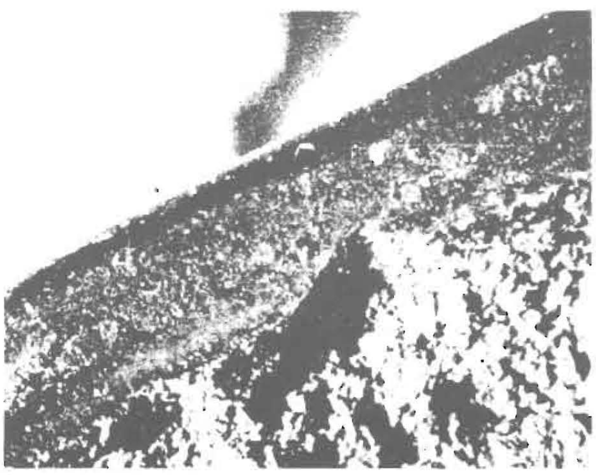

FIGURE 3. CORROSION PITS ON ROOT HOOK NEAR FRACTURE INITIATION SITE.

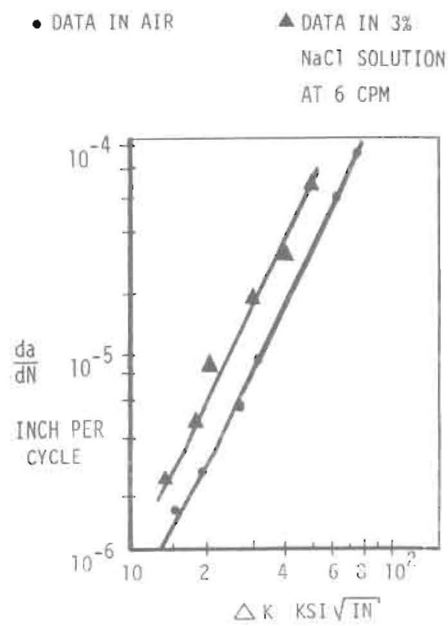

FIGURE 4. CRACK GROWTH DATA FOR 304 STEEL IN AIR AND 3 PERCENT NAOH SOLUTION (BARSOM,NOVAK,REF 20).

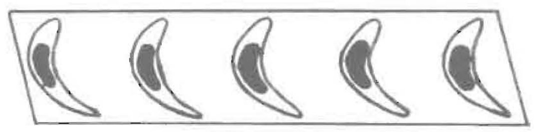

FIGURE 5. MEDIUM-PRESSURE BLADE PROFILES IN AXIAL-FLOW TURBINE STAGE.

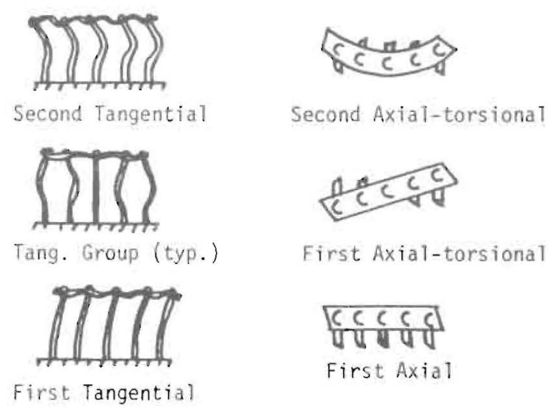

FIGURE 6. MODE SHAPES OF TURBINE BLADES IN GROUPS.

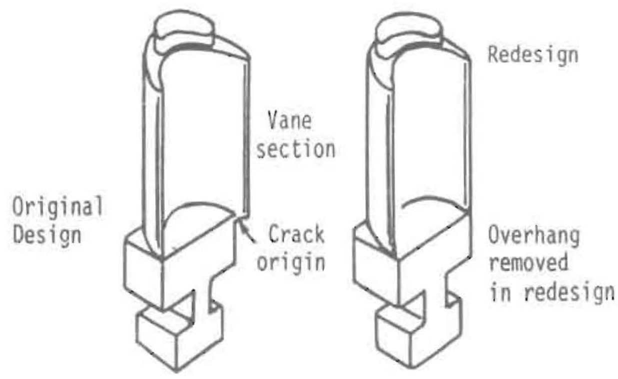

FIGURE 7. DETAIL OF FAILED BLADE AND MODIFIED REPLACEMENT BLADE, VANE OVERHANG REGION.

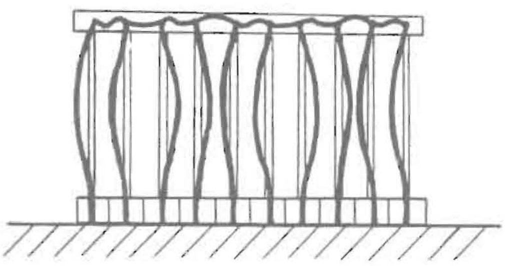

FIG. 8(a): SECOND TYPE TANGENTIAL GROUP MODE

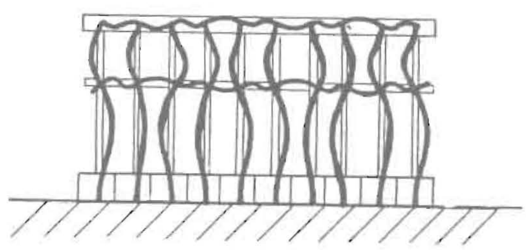

FIG. 8(b): SECOND TYPE TANGENTIAL WITH TIE WIRE

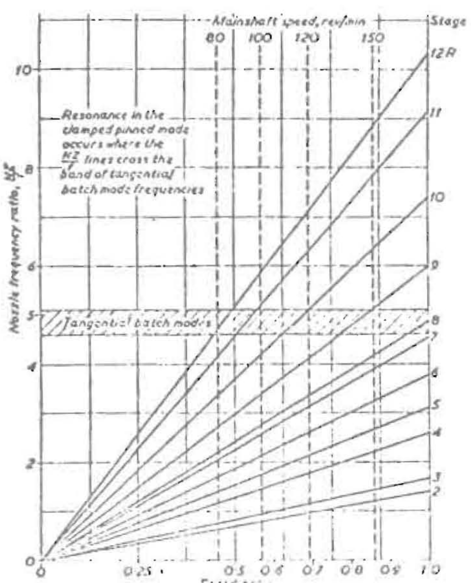

FIGURE 9. CAMPBELL DIAGRAM FOR FATIGUED MARINE TURBINE BLADE (FLEETING,COATS,REF.13).

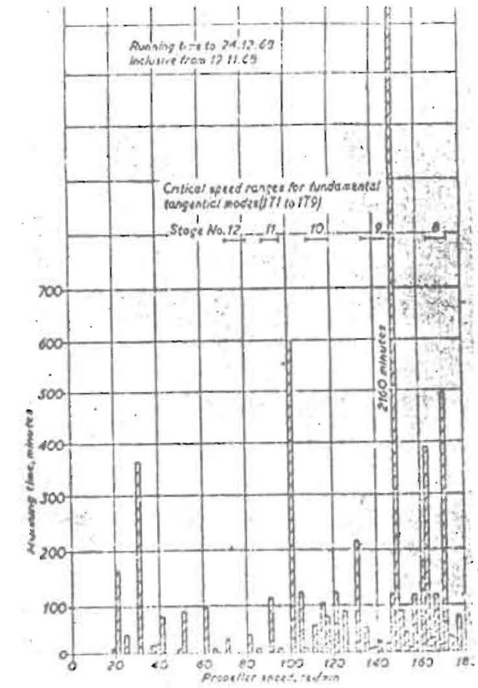

FIGURE 10. TURBINE LOG. TIMES AT VARIOUS SPEEDS. (FLEETING,COATS REF. 13).

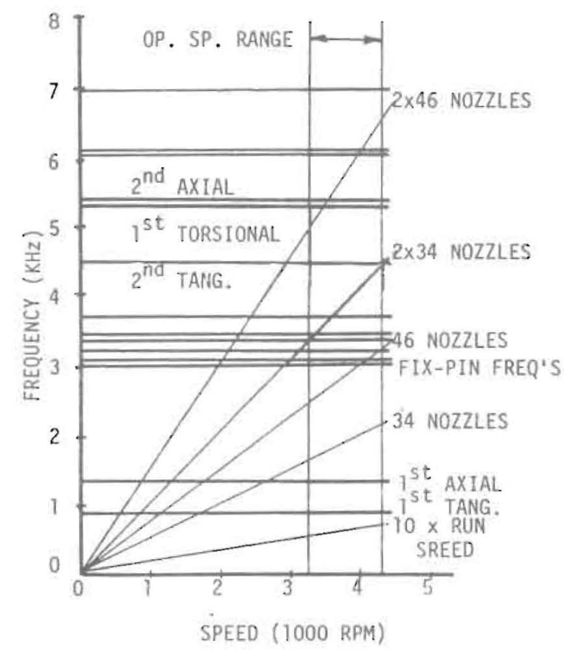

FIG. 11(a): CAMPBELL DIAGRAM FOR FAILED BLADES

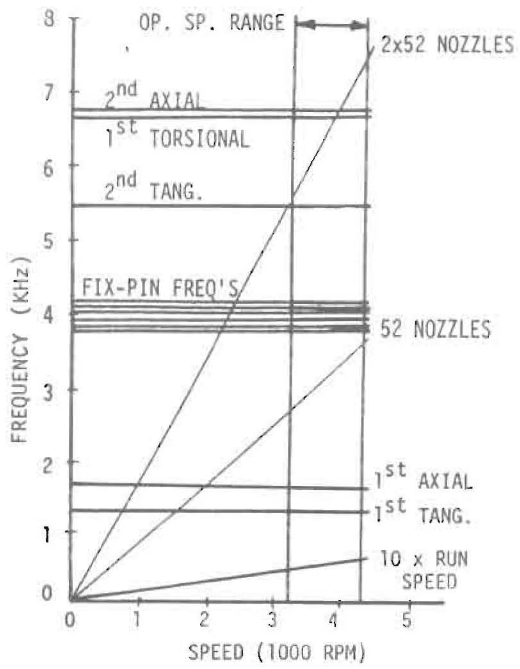

FIG. 11(b): CAMPBELL DIAGRAM FOR REPLACEMENT BLADES

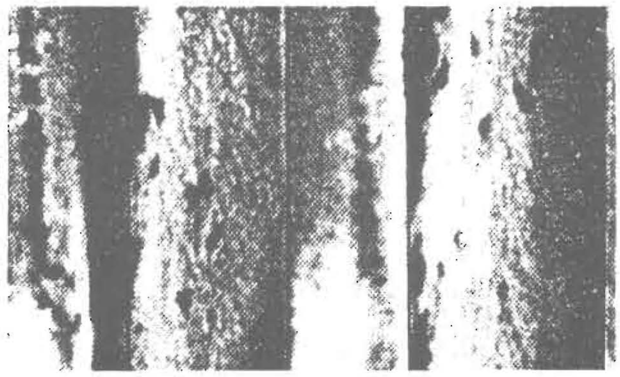

FIGURE 13. BLADE VANE SECTIONS SHOWING WHITE CHEMICAL COATINGS.

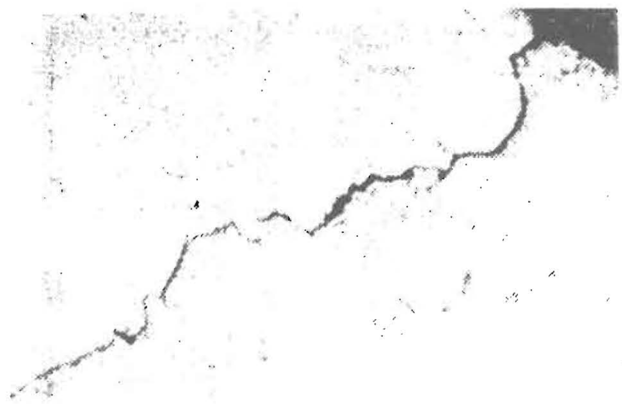

FIGURE 14. CRACK ORIGIN AND PROPAGATION FROM STRESS RAISER INTO COMPONENT.

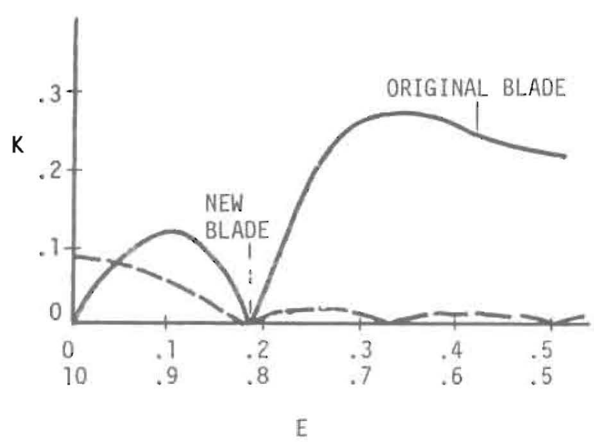

FIG. 12: RESONANT RESPONSE FACTOR REDESIGN

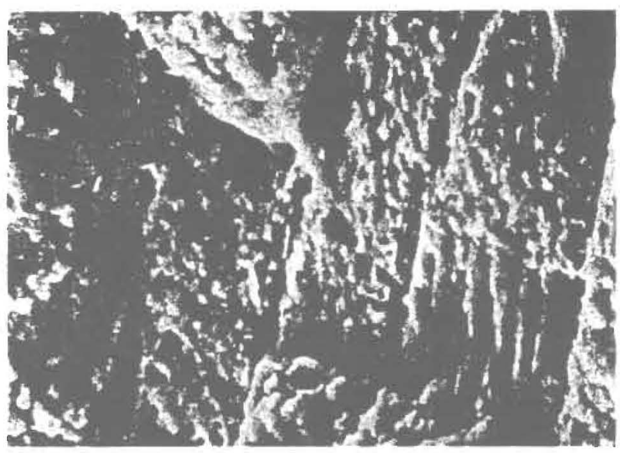

FIGURE 15. ELECTRON MICROGRAPH SHOWING NAOH NODULES ON SURFACE OF CRACK.

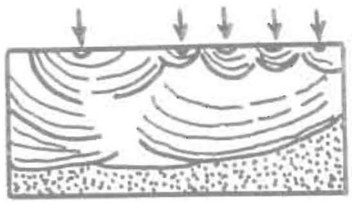

FIGURE 16. MULTIPLE ORIGIN CRACKING.

FIGURE 17. CRACK PATH. STRAIGHT, INTERGRANULAR.

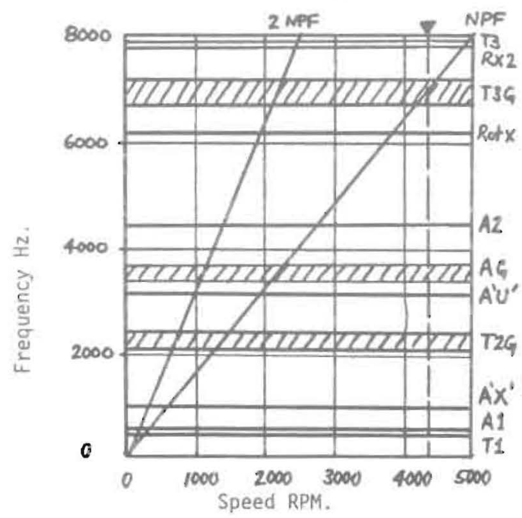

FIGURE 19. CAMPBELL DIAGRAM, 4TH STAGE, 96 NOZZLE DIAPHRAGM. FAILED ROW.

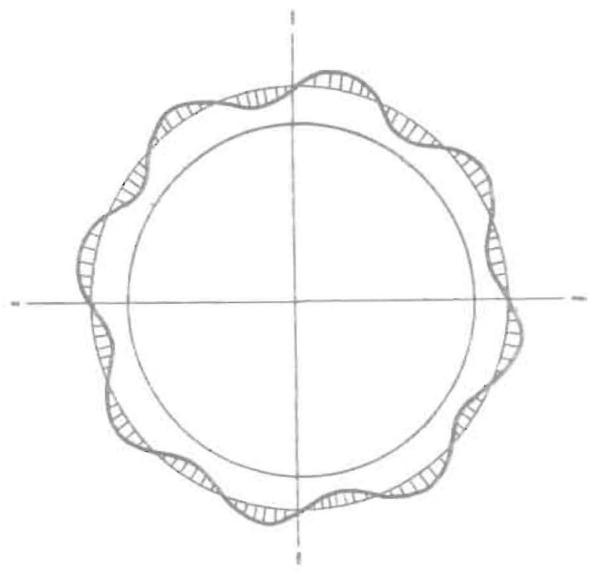

(a) EIGHT-PER-REV HARMONIC EXCITATION AROUND NOZZLE CIRCUMFERENCE.

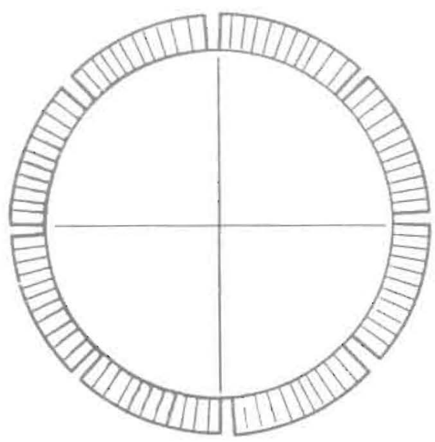

(b) LONG-ARC SHROUDS EACH SPANNING ONE EXCITATION WAVE AT ALL POSITIONS.

FIGURE 18. PRINCIPLE OF LONG-ARC SHROUD.